Strain-Rate Dependent Pre-Failure, Failure and Post-Failure Behavior of Shale: Experiments and Modeling

Marte Gutierrez[1] and Zhenkun Hou[1,2]

[1]Department of Civil and Environment Engineering, Colorado School of Mines, Golden, CO 80401, USA
[2]School of Resource and Environment, North China University of Water Resources and Electric Power, Zhengzhou, 450045, China

ABSTRACT

The strain rate dependent mechanical behavior of shale was extensively characterized using triaxial compression tests carried out at different axal strain rates. Based on the experimental results, a constitutive model for shale under different rates of loading was proposed. The model is based on a combination of viscoelasticity and damage mechanics and is formulated to predict the brittle behavior of shales from the pre-peak stage, peak and post peak strain softening regimes. Shear failure and strain softening are attributed to damage due to the growth of fractures in the shale, and de-bonding and decohesion mechanisms responsible for the fracture evolution. Damage is described by a scalar variable D and is assumed to commence when the stress-strain behavior deviates from linear elasticity. It was found that damage evolution during shearing in shale can be adequately represented probabilistically using a Weibull probability distribution function based on the axial strain level. An empirical axial strain rate dependent Young's modulus, together with the damage evolution law, completes the viscoelastic damage model. The model is shown to adequately represent the complete stress-strain response of shale at different axial strain rates and to predict the axial strain rate dependent shear strength of shale.

Introduction

Improved understanding of the mechanical behavior of shales is one of the important challenges in the geomechanics community as shales are often encountered in many civil, energy, environmental and nuclear engineering applications. In energy engineering, the development of modern technologies in drilling and fracturing has transformed oil and gas-bearing shale from an otherwise uneconomic material to a profitable energy resource (Mahanta et al. 2016; Middleton et al. 2015). There is a wealth of knowledge on the mechanical properties of shale. The deformation, tensile and shear strength, brittleness/ductility, and fracturing of shale have been widely studied using Brazilian, uniaxial and triaxial compression tests under different loading conditions (e.g. Dewhurst and Hennig, 2003; Nygaard et al., 2015; Ayatollahi and Mishra, 2017).

Most of the studies on shale have been conducted with constant quasi-static loading rate. Previous studies have shown there is a clear time effect on many non-shale rocks. Experimental investigations show that increasing strain rate increases the peak shear strength and elastic modulus of many non-shale rocks, such as sandstone, limestone and tuff. While there is a growing body of knowledge on shale mechanical behavior, there remains a relatively limited number of studies addressing the strain rate-dependent mechanical behavior of shale. At the same time, knowledge and understanding of the effects of strain rate on shale is important in many applications.

Another major challenge is the modeling of the post-peak behavior of shales. Several constitutive models for shales have been proposed (e.g. Zhao, 2000; Franchesco et al., 2015), but almost all of these models are valid only for the pre-peak and peak behavior of shales. The most common approach is to use plasticity theory and employ elasticity, and yield/failure criteria, plastic potential and hardening function to formulate the model. Strain softening behavior following failure is problematic to handle in plasticity theory as it requires a negative hardening modulus, which can lead to violation of thermodynamic principles. As a result, almost all constitutive models for shales assumes only strain hardening or perfect plasticity at failure. It is essential to be able to predict response all the way to post-peak strain softening to faithfully model the geomechanical response of shale over a wide strain region.

Strain-Rate Dependent Behavior of Shale from Experiments

Triaxial compression tests were conducted on specimens taken from a fresh black shale outcrop in the Longmaxi Formation in Dayou Town of Nanchuan District, Chongqing City, China. The outcrop belongs to the Lower series of Silurian, and is a natural extension of the shale gas reservoir in the Fuling District of Chongqing. Undrained loading was carried out on horizontal specimens of the shale at a constant confining pressure of σ_3 equal to the in situ vertical stress of 50 MPa, and at different axial strain rates $\dot{\varepsilon}_1$ of $5\times10^{-6}s^{-1}$, $1\times10^{-5}s^{-1}$, $1\times10^{-4}s^{-1}$, $5\times10^{-4}s^{-1}$ and $1\times10^{-3}s^{-1}$.

As shown in Figure 1, the deviatoric stress $(\sigma_1-\sigma_3)$ vs. axial strain ε_1 curves of Longmaxi shale at different axial strain rates can be divided into the initial compression stage (due to closure of microfractures from sampling-induced damage of the test specimens), the elastic stage, the yield stage, peak point, and the post peak strain softening to the residual stage. Overall, the greater the strain rate $\dot{\varepsilon}_1$ the higher the elastic modulus, peak strength and residual strength. On the other hand, despite of the change in the strain rates of more than 10^3 times, the axial strain values at linear elastic yield are almost the same at about 0.6%. Similarly, the axial strains at the peak points are observed to be about 1% for all tests. From the strong strain softening and post-peak slopes of stress-strain curves, it can be seen that all shale samples show brittle characteristics regardless of the strain rate.

The strain-rate dependent stress-strain response of shale are shown in Figure 2 in terms of the elastic modulus *E*, based on the linear portion of the stress-strain curves, as function of the strain rate $\dot{\varepsilon}_1$ in a *E*–log($\dot{\varepsilon}_1$) plot. As can be seen, as the strain rate $\dot{\varepsilon}_1$ increases, there is a definite increase in elastic modulus *E*. The mean values of *E* have an exponential function relationship with $\dot{\varepsilon}_1$, as represented by the correlation equation given in Figure 2. The peak shear strength $(\sigma_1-\sigma_3)_{max}$ as function of the strain rate $\dot{\varepsilon}_1$ is also shown in Figure 2. Higher strain rates lead to higher peak strength, which indicates that axial strain rate $\dot{\varepsilon}_1$ has a strengthening effect on the shale. Similar to the elastic modulus, an exponential relationship exists between the mean values of $(\sigma_1-\sigma_3)_{max}$ and $\dot{\varepsilon}_1$, which can be fitted by the by the regression equation inserted in the figure.

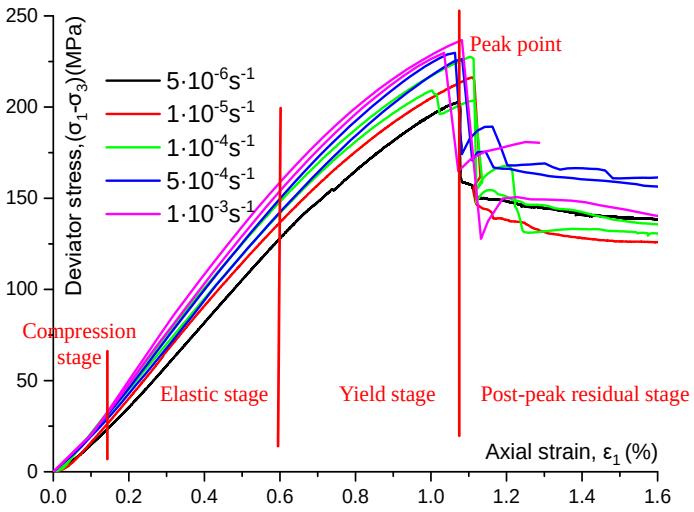

Figure 1. *Deviatoric stress vs. axial strain curves for Longmaxi shale sheared at different axial strain rates under constant* σ_3 *=50 MPa triaxial conditions.*

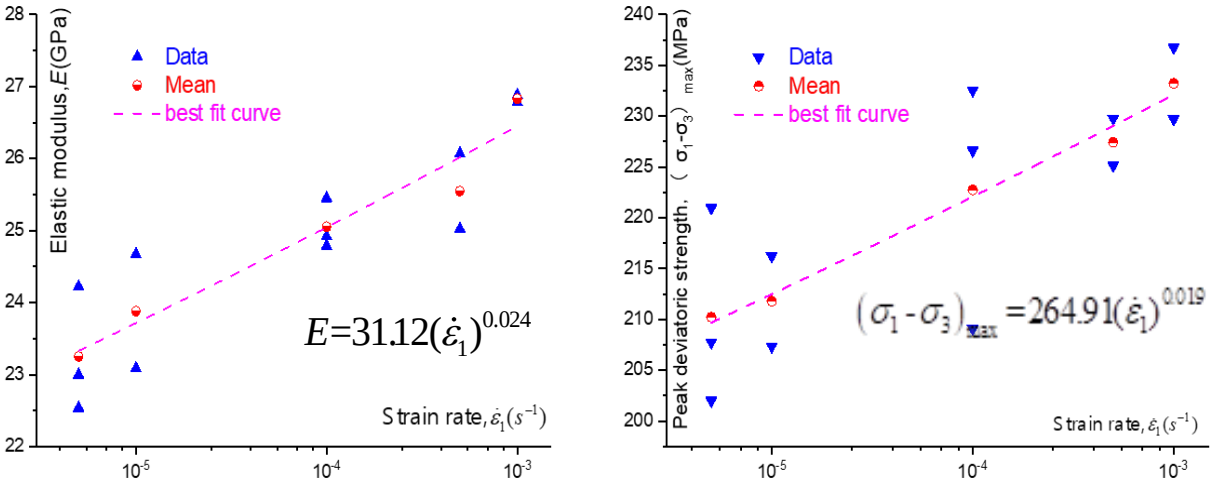

Figure 2. *Strain-rate dependent Young's modulus (left) and peak deviatoric shear strength (right) of Longmaxi shale. Best fit equations are embedded in the figures.*

The failure patterns of the test specimens under triaxial compression at different strain rates are shown in Figure 3. For $\dot{\varepsilon}_1 \le 1\cdot10^{-5}s^{-1}$, a typical single shear failure is formed and the shear plane runs through the whole sample with some visible shear displacement. The angle between the failure surface and horizontal axis is in the range of 66°~74°. For $\dot{\varepsilon}_1 > 1\cdot10^{-5}s^{-1}$, the fracture morphology of shale is more complex, the number of shear fracture planes increases significantly, some of bedding planes are opened by localized tensile stress caused by sliding along the shear fractures, and there are many fine vertical cracks between the shear fracture surfaces. Under high strain rates, the fracture morphology shows simultaneous development of multiple microcracks, resulting in the destabilization of shale and increased damage, eventually forming a complex crisscrossing fracture network.

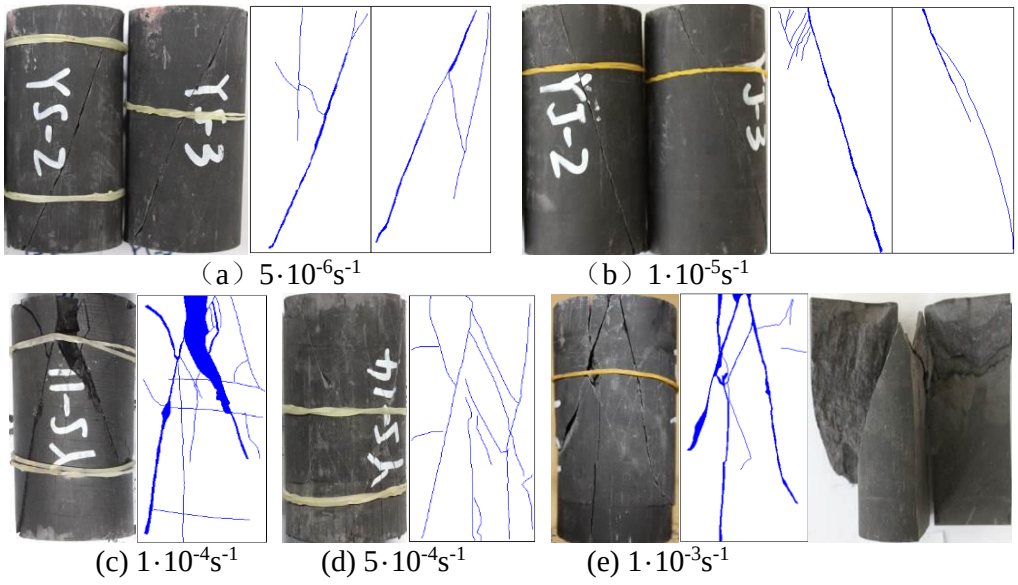

Figure 3. *Fracture geometries of failed samples of Longmaxi shale sheared under different axial strain rates in triaxial compression.*

Modeling of the Strain-Rate Dependent Behavior of Shale

To simulate the strain-rate dependent stress-strain behaviour of shale spanning the pre-peak, peak and post-peak regions, a viscoelastic damage model was developed with the following elements: 1) A strain-rate dependent elastic modulus directly based on Figure 2, and 2) A damage formulation based on Weibull probability distribution of failure-induced fracturing in shale. Damage starts at yielding when the stress-strain curve deviates from linear elasticity and is a function of axial strain above yield strain. The damage evolution is directly curve-fitted from the experimental results. The resulting model formulation is very compact and can be expressed by two simple expressions:

1) Before damage occurs when the axial strain ε_1 is less than or equal to the yield axial strain ε_{1y}, the stress-strain curve is expressed by the viscoelastic relation:

$$\left(\sigma_1-\sigma_3\right)=E_o\left(\dot{\varepsilon}_1\right)^n\varepsilon_1 \tag{1}$$

2) After damage occurs when the axial strain ε_1 exceeds the yield axial strain ε_{1y}, the stress-strain curve is expressed by the viscoelastic damage relation:

$$\left(\sigma_1-\sigma_3\right)=E_o\left(\dot{\varepsilon}_1\right)^n\left\{\varepsilon_{1y}+\exp\left[-\left(\left(\frac{\varepsilon_1-\varepsilon_{1y}}{\varepsilon_o}\right)^m\right)\right]\right\}\left(\varepsilon_1-\varepsilon_{1y}\right) \tag{2}$$

In the above equations, *n* is the exponent for the axial strain rate-dependent Youngs modulus, E_o is the reference Young's modulus, *m* is the Weibull modulus, and ε_o is the Weibull reference strain.

Figure 4 shows the predicted stress-strain response of Longmaxi shale under the same loading conditions shown in Figure 1. By comparing Figures 1 and 4, it can be seen than the model is able to satisfactorily predict the strain-rate dependent stress-strain response of shale from pre-peak, peak to post-peak regimes. In addition, it is possible to show that the viscoelastic damage model analytically predicts the following strain-rate dependent peak shear strength:

$$\left(\sigma_1-\sigma_3\right)_{\max}=C\cdot E_o\left(\dot{\varepsilon}_1\right)^n \tag{3}$$

where $C=\exp\left(-1/m\right)\varepsilon_o m^{-1/m}+\varepsilon_{1y}$. Comparison of the axial strain-rate dependent peak shear strength $(\sigma_1-\sigma_3)_{\max}$ predicted from Equation (3) with the experimental data is shown in Figure 5. As shown in the figure, the analytically predicted shear strength based on the model parameters E_o, *n*, *m*,

ε_{1y} and ε_o compares well with the experimental data and the best-fit curve through the experimental data.

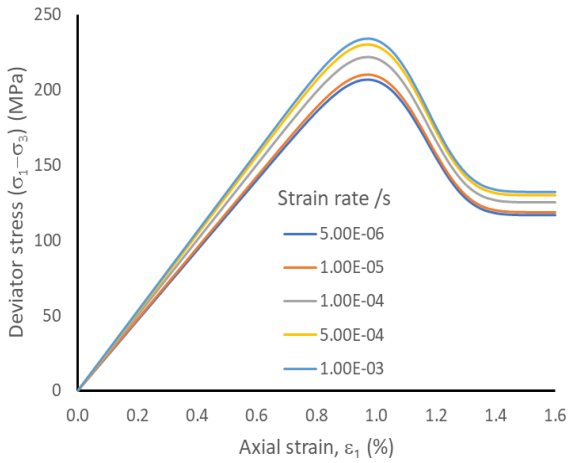

Figure 4. *Predicted shear stress strain curves for different axial strain rates.*

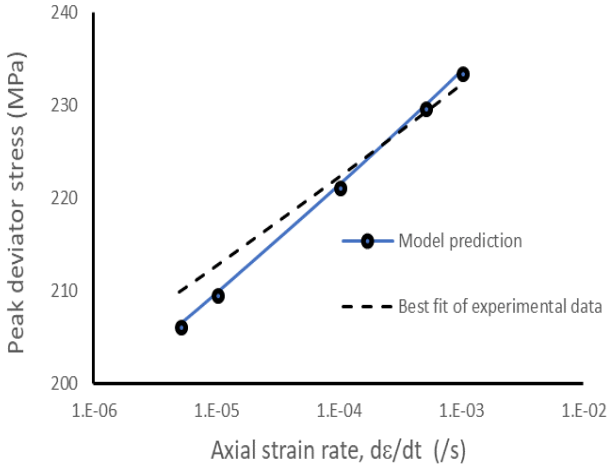

Figure 5. *Comparison of analytically predicted stain-rate dependent peak shear strength against experimental results.*

Conclusions

Experimental results using triaxial compression tests at constant σ_3 =50 MPa showed the distinct effects of axial strain loading rate on the stress-strain response of Longmaxi shale from pre-peak, peak and post-peak strain localization regimes. Axial strain rate also affected the fractured geometry of the tested samples after failure. Based on the experimental results, a viscoelastic damage model was developed using a strain-rate dependent elastic modulus and a damage formulation based on Weibull probability distribution of failure-induced fracturing in shale. Damage starts at yielding when the stress-strain curve deviates from linear elasticity and is a function of axial strain above yield strain. Model predictions satisfactorily agree with experimental results on Longmaxi shale.

References

Arora, S. and Mishra, B. [2017]. Investigation of the failure mode of shale rocks in biaxial and triaxial compression tests. *International Journal of Rock Mechanics and Mining Sciences*, **79**, 109-123.

Ayatollahi, M.R. and Aliha, M.R.M. [2008]. On the use of Brazilian disc specimen for calculating mixed mode I–II fracture toughness of rock materials. *Engineering Fracture Mechanics*, **75**(16), 631-4641.

Dewhurst, D.N. and Hennig, A.L. [2003] Geomechanical properties related to top seal leakage in the Carnarvon Basin, Northwest Shelf, Australia. *Petroleum Geoscience*, **9**(3), 255-263.

Francesco, P., Sergio, S. and Lyesse, L. [2015] Constitutive analysis of shale: a coupled damage plasticity approach. *International Journal of Solids and Structures*, **75-76**, 88-98

Mahanta. B., Tripathy, A., Vishal, V., Singh, T.N. and Ranjith, P.G. [2016] Effects of strain rate on fracture toughness and energy release rate of gas shales. *Engineering Geology*, **218,** 39-19.

Middleton, R.S., Carey, W.J., Currier, R.P., Hyman, J.D., Kang, Q., Karra, S., Jiménez-Martínez, J., Porter, M.L. and Viswanathan, H.S. [2015] Shale gas and non-aqueous fracturing fluids: opportunities and challenges for supercritical CO2. Applied Energy, **147**(3), 500-509.

Nygaard, R., Gutierrez, M., Brattli, R.K. and Høeg, K. [2005] Brittle-ductile transition, shear failure and leakage in mudrocks from the North Sea and adjacent areas. *Marine and Petroleum Geology*, **23**, 201-212.

Zhao, J. [2000] Applicability of Mohr–Coulomb and Hoek–Brown strength criteria to the dynamic strength of brittle rock. *International Journal of Rock Mechanics and Mining Sciences*. **37**(7), 1115-1121.